National Radio Astronomy Observatory
Tucson, Arizona

February 20, 1987

MEMORANDUM

To: D. T. Emerson, J. W. Findlay, R. W. Freund, J. W. Lamb,
J. M. Payne, E. B. Stobie, and 345 GHz Observers

From: P. R. Jewell

Subject: Report of 345 GHz Receiver Tests, 1987 Feb. 16-18

This memo gives a description of the tests performed with the 345 GHz receiver. Many of the tests need follow-up work and many of the (tentative) conclusions need more thought; I hope that this memo may provoke some discussion.

The participants in the tests were DTE, JMP, EBS, and myself. The observations were made with the J = 3-2 CO line (345.796 GHz, 0.871 mm wavelength) in the upper sideband. We performed the following tests:

1) Receiver properties;
2) Aperture efficiency measurement;
3) Map of the main diffraction beam;
4) Map of the error beam;
5) Measurement of gain vs. North-South translation stage position; and
6) Measurement of sky noise as a function of subreflector throw.

1. Receiver Properties

The receiver is a single channel mixer with Gunn oscillator and a Millitech quadrupler. After some initial phase lock problems on the first night, the receiver and LO system performed extremely well. The DSB receiver temperature was 1000 - 1100 K, as measured with hot/cold loads on the telescope. The gain of the receiver is fairly stable with elevation changes; with the vane over the feed, the total power response shows only a small change at high elevation.

2. Aperture Efficiency Measurement

The aperture efficiency was measured on 17 Feb. with a total power ON/OFF measurement of Saturn. Assuming a beam size of 20", and a disk brightness temperature of 140 K, the flux density of Saturn at 344.3 GHz was 1672.9 Jy. The atmospheric zenith optical depth was measured to be 1.13 by a hot/cold/sky measurement (the

SPTIP routine systematically underestimates the optical depth, and breaks down badly for high tau). The total power antenna temperature, corrected for the atmosphere, was 8.0 K as measured through the digital backend. The calibration scale of the DBE was measured with a hot/cold load.

The resulting aperture efficiency is 11.6 %. I don't have a formal error for this number, but it could be 4 or 5 percentage points. The total power scan was noisy and the atmosphere was bad (the zenith optical depth may not accurately characterize the opacity at the position of observation). Last year, we measured 14 % aperture efficiency at 345 GHz; I consider these measurements the same within the errors.

3. Map of the Main Diffraction Beam

The Saturn beam map is shown in Figure 1. The map was made in the dual-beam mode with a 1' beam throw. The displayed map has been restored and baselined. The cell size of the map was 7" and the integration time per point was 3 sec.

The map is fairly noisy. The lowest contour around the beam is -8 dB of the maximum intensity. The highest contour on the map away from the beam is -6 dB. We can conclude that no sidelobes are higher than -6 dB.

The most interesting characteristic of the map is the azimuth elongation of the beam, and the beam widths: the azimuth FWHP is 21.6" and the elevation width is 15.0". At this wavelength, lamda/D = 15". The diameter of Saturn was 15.3". Correcting for the broadening of the beam by the source, (Az) = 19.6" and (El) = 12". Thus, the elevation width is narrower than theoretically possible for even a uniformly illuminated dish.

Question #1: Why is the beam elongated in azimuth? (This effect is also seen at other frequencies.)

Question #2: Why is the elevation FWHP so small? (Noise in the map is a prime possibility.)

4. Measurement of the Error Pattern

We measured the extent and amplitude of the error pattern in one dimension by taking azimuth cross scans onto a nearly full moon. The scan was made with the digital backend and with the subreflector locked. The angular length of the scan was 33', scanning from a negative azimuth offset and ending at approximately the center of the moon's disk. The step size was 40". The scan is shown in Figure 2 and the differentiation of that scan, which gives the beam pattern, is shown in Figure 3.

In Figure 3, the center spike is the underresolved main beam and the broad pedestal is error beam. The parameters from the two-Gaussian fit are

	Amplitude	FWHP
Main Beam Fit	30.315	48.25'
Error Beam Fit	9.119	5.64'

The amplitudes are uncalibrated antenna temperatures and must be reduced as described below. The interpretation of these results require some care. Since the scan was onto an extended source, each point on the 1-D plot is actually an integration of a strip from the circular response of the beam and a strip from the moon's disk, as shown below.

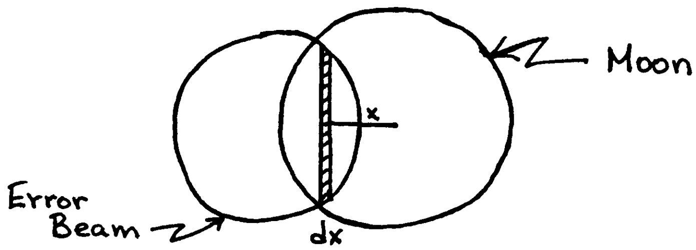

DTE and I convinced ourselves that the fraction of power in the main beam relative to the error beam is given by the area under the 1-D profile, i.e., the power contained in the error pattern is given by $A\theta$ rather than the usual $A\theta^2$. Hence, the proper amplitudes of the main and error beams should be scaled down by $1/\theta$ from the fitted values. If we normalize the sum of the amplitudes to 1 (i.e., $A_M + A_E = 1$), then

$$A_M = \frac{A_m/\theta_M}{A_m/\theta_M + A_e/\theta_E} = 0.959 \; , \qquad (1)$$

and

$$A_E = \frac{A_e/\theta_E}{A_m/\theta_M + A_e/\theta_E} = 0.041 \; , \qquad (2)$$

where A_m and A_e are the amplitudes given by the Gauss fit. The fraction of power in the main beam relative to the error beam is thus given by

$$\eta_{M*} = \frac{1}{1 + \dfrac{A_E\,\theta_E^2}{A_M\,\theta_M^2}} = 0.32 \; . \qquad (3)$$

This number can be used to help calibrate spectral line data taken with chopper wheel calibration (T_R^* scale): it is the efficiency by which observations of a point (or spatially confined) source should be scaled, assuming no coupling with the error pattern. (This last assumption leads to a small error because of the amplitude of the error pattern is non-neglibible.) The number is also an upper limit on the aperture efficiency. If we scale this number down by the rear spillover efficiency (~0.85), the forward spillover efficiency (~0.75), and the reduction in effective aperture because of feed taper (~0.60), we get a calculated aperture efficiency of 12 %, which is good agreement with the directly measured value.

We can also apply Ruze theory to the error beam parameters. The correlation scale size of antenna surface deviations is given by

$$c = 2(\ln 2)^{1/2} \frac{\lambda}{\pi \theta_E} = 28 \text{ cm} . \quad (4)$$

In addition, we can estimate the rms surface accuracy from the error pattern measurement. The Ruze relation for this is

$$\frac{A_E\, \theta_E^2}{A_M\, \theta_E^2} \, \frac{\eta_{A0}\, \pi^2\, K^2}{16 \ln 2} + 1 = \exp\left(\frac{4\pi\sigma}{\lambda}\right)^2 , \quad (5)$$

where η_{A0} is the infinite wavelength aperture efficiency (about 0.52) and K is the taper function (about 1.2). The resulting rms surface accuracy σ = 65 μm. This number is somewhat lower than expected, as our radiometric extrapolation of aperture efficiencies gives about 75 μm. The aperture efficiency extrapolation may also be subject to errors (e.g., Cassegrain vs. prime focus efficiencies and proper adjustment of the N-S translation stage at high frequencies). We need to give this result further consideration.

5. Measurement of Optimum North-South Translation Stage Position

According to Lee King's model of the 12 m, the position of the prime focus will move in the North-South direction as the telescope changes elevation because of feed leg sag. The effect is predicted to be quite strong at high frequencies. Despite several previous attempts, we've never been able to accurately measure the optimum position of the N-S stage (which suggests that the effect is smaller than predicted). Part of the problem has been that, since the elevation pointing changes with N-S stage position, the measurement has been tedious and lengthy. The pointing must be redetermined at each setting which means that a single measurement has taken 20-30 min. During this time, changes in the atmosphere or receiver can mask the effect. To overcome this problem, we have carefully calibrated the change in elevation pointing as a function of N-S position and EBS has developed an automatic N-S focus routine called NSFOCAL. NSFOCAL drives the N-S stages in 1 mm steps between -3 and +3 mm and automatically adjusts the elevation pointing. NSFOCAL takes less than 5 min to execute and is reduced in an analagous way to the radial focus routine FOCALIZE.

The first measurements with NSFOCAL are shown in Figure 4. The measurements were all noisy, particularly those at low elevation, which should probably be ignored. The peak amplitudes are clustered around +1 mm and were typically 10-20 % stronger than at 0 mm. The elevation range covered was too narrow to discern any elevation effects. The observations were made on Jupiter, which had a 35" diameter (1.5 times the FWHP of the main beam) at the time of observation. The source was thus less than ideal, but was the only reasonable candidate because of its strength. The pointing constant used was +34"/mm, which had been measured last July. We confirmed that this number was still accurate, as shown in Figure 5.

We did not feel that the measurements were sufficiently reliable to change the N-S position for general observations. Clearly, the calibration of this stage needs more attention. Now that the NSFOCAL routine is working, we may be able to more accurately measure the effect at 230 GHz, where the sky has less attenuation and the receiver is more sensitive.

6. Measurement of Sky Noise as a Function of Subreflector Throw

We found that the switched power noise of the system was critically dependent on the angular throw of the subreflector: the sky noise increased by about a factor of 2 between a 1' and 2' beam throw. A crude graph of the effect, measured from the chart recorder, is shown in Figure 6. This effect is presumably results when the near-field beam columns of the two switch positions begin to diverge as they pass through the atmosphere. It is quite possible that the measured effect will change with atmospheric conditions. At the time of observation, the sky was clear and stable to the eye. For now, we recommend a 1' beam throw for continuum observations.

FIGURES

Figure 1: 345 GHz beam map against Saturn. The map was made in dual beam mode and has been restored and baselined. The cell size of the map was 7".

Figure 2: An average of numerous azimuth cross scans onto the moon's disk. The map was made with the subreflector fixed. The step size was 40".

Figure 3: A differentiation of the scan shown in Figure 2. The central spike is the underresolved main beam and the broad profile is the error pattern.

Figure 4: A plot of optimum North-South translation stage position as a function of elevation. The measurements were made using the NSFOCAL routine for automatically moving the N-S stage and adjusting elevation pointing. All the measurements were noisy, particularly those at low elevation.

Figure 5: Change in elevation pointing with North-South translation stage position.

Figure 6: A plot of switched power sky noise as a function of subreflector throw (measured off the chart recorder).

TITLE SATURN AT 3[redacted]GHZ 17 FEB 1987

LOWEST C[redacted]UR -2000
CONTOUR INTERVAL 2000
MAP PEAK 18832

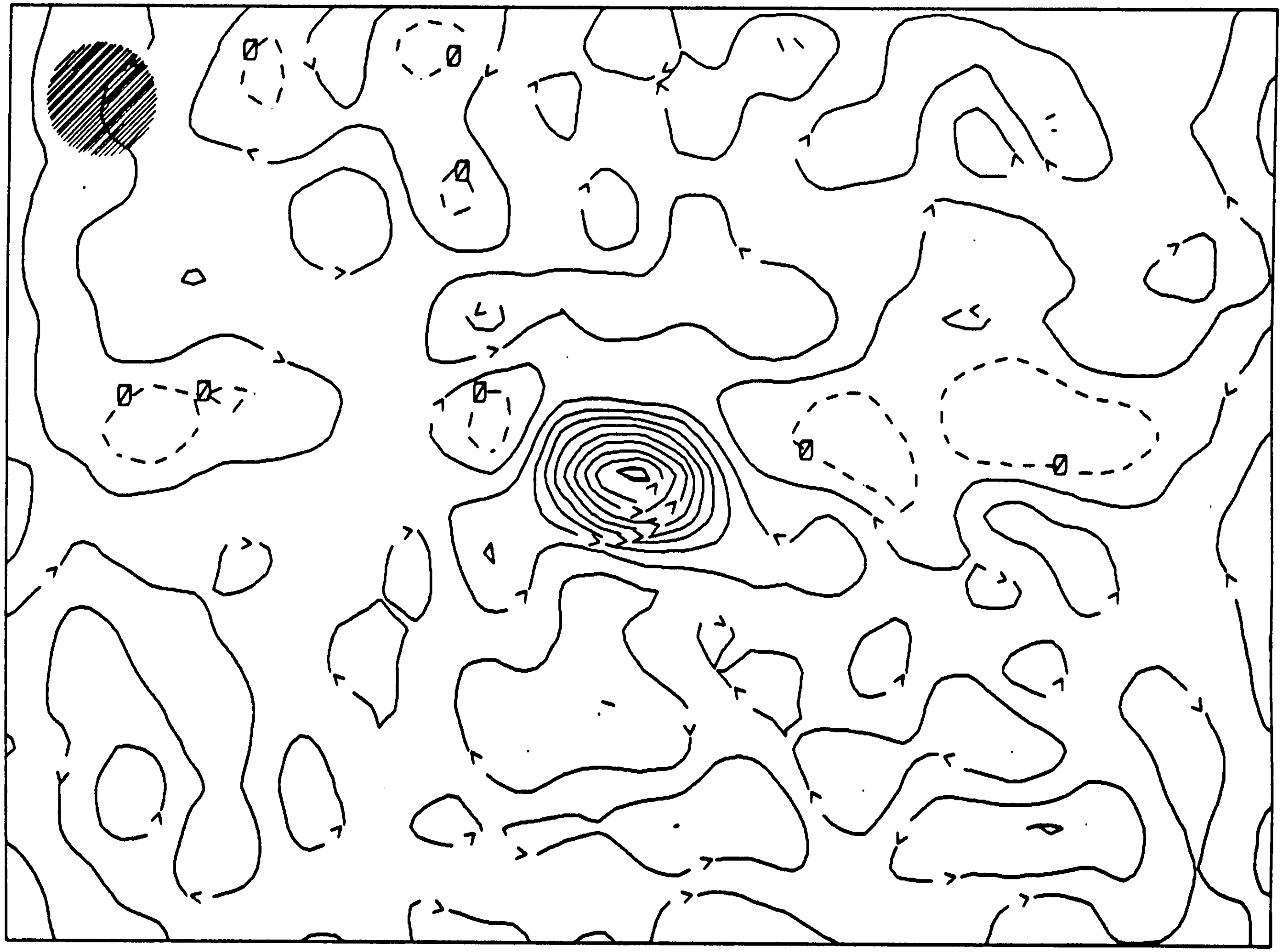

AZ WIDTH = 0.′36 = 21.″6

EL WIDTH = 0.′25 = 15.″0

θ_{SAT} = 15.″3

FIG. 1

SCAN	SOURCE	#CH	DATE	[illegible]	SEC	TS	AZ	EL
2386	MOON	1	2-17	12 10 37	5.0	200	169.6	54.

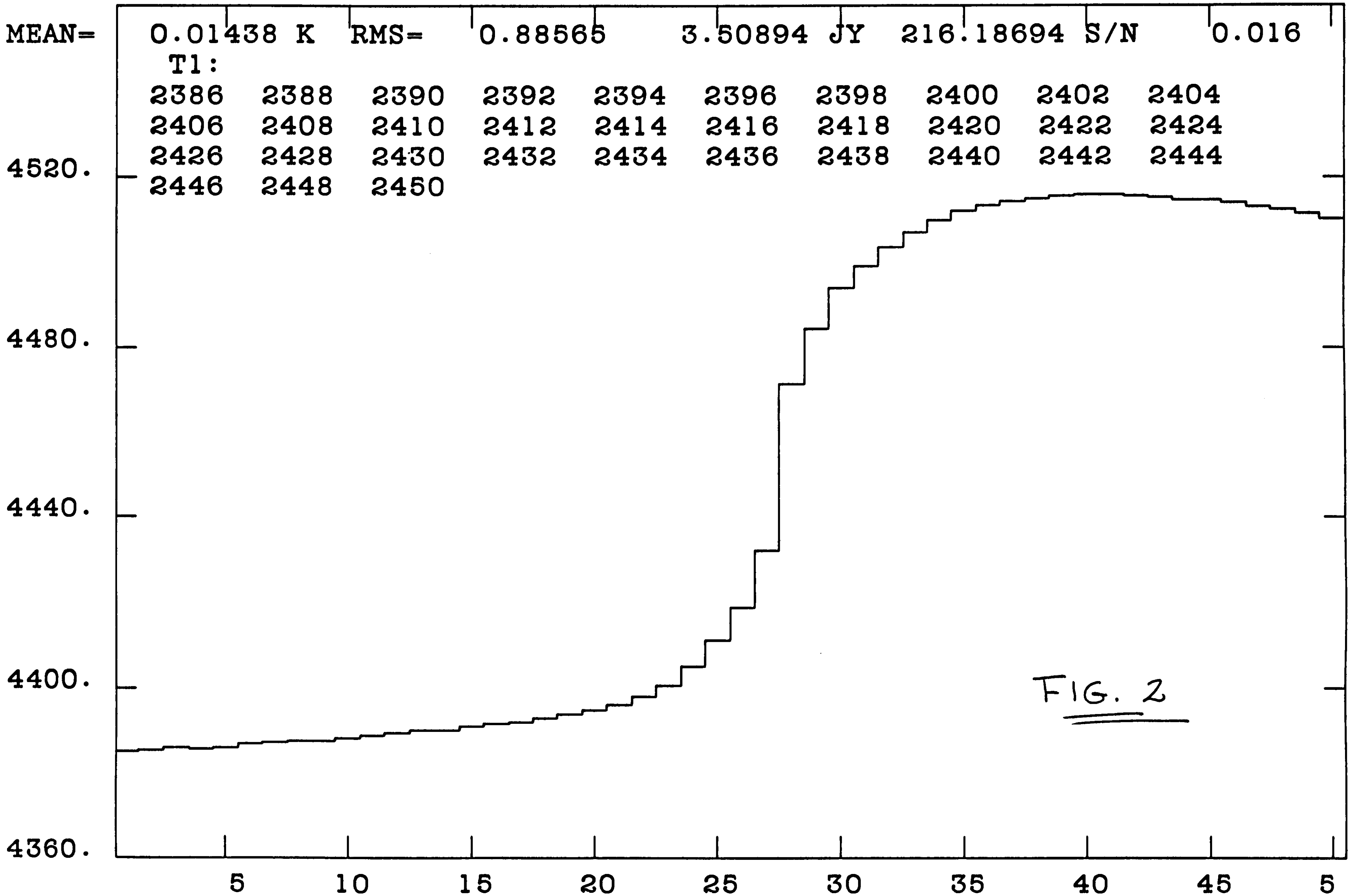

FIG. 2

SCAN	SOURCE	#CH	DATE	LST	SEC	TS	AZ	EL
2386	MOON	1	2-17	12 10 37	5.0	200	169.6	54.

TA= 0.0144 0.8856 JY= 3.509 216.187 S/N= 0.02 ASF=3.25

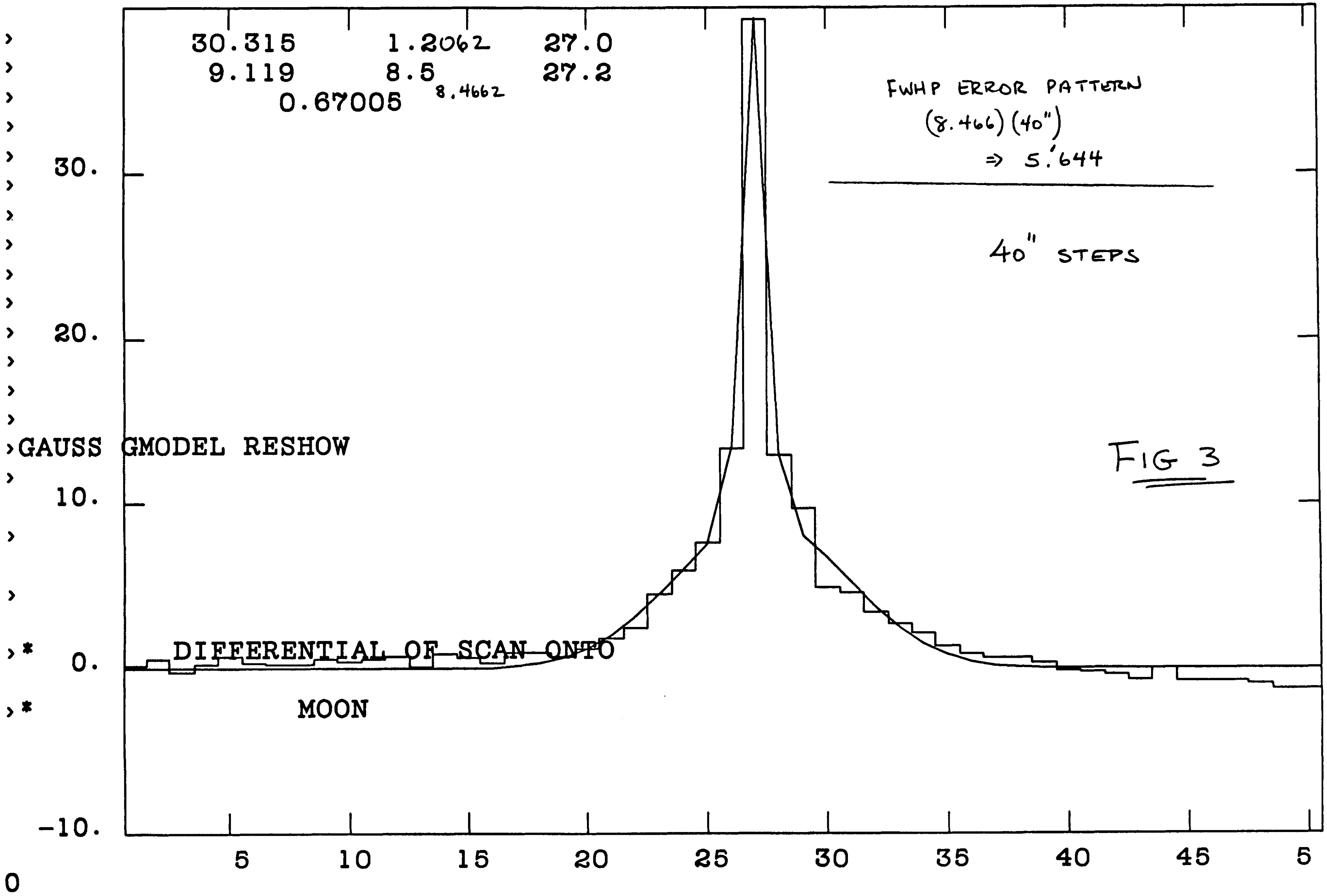

FIG 3

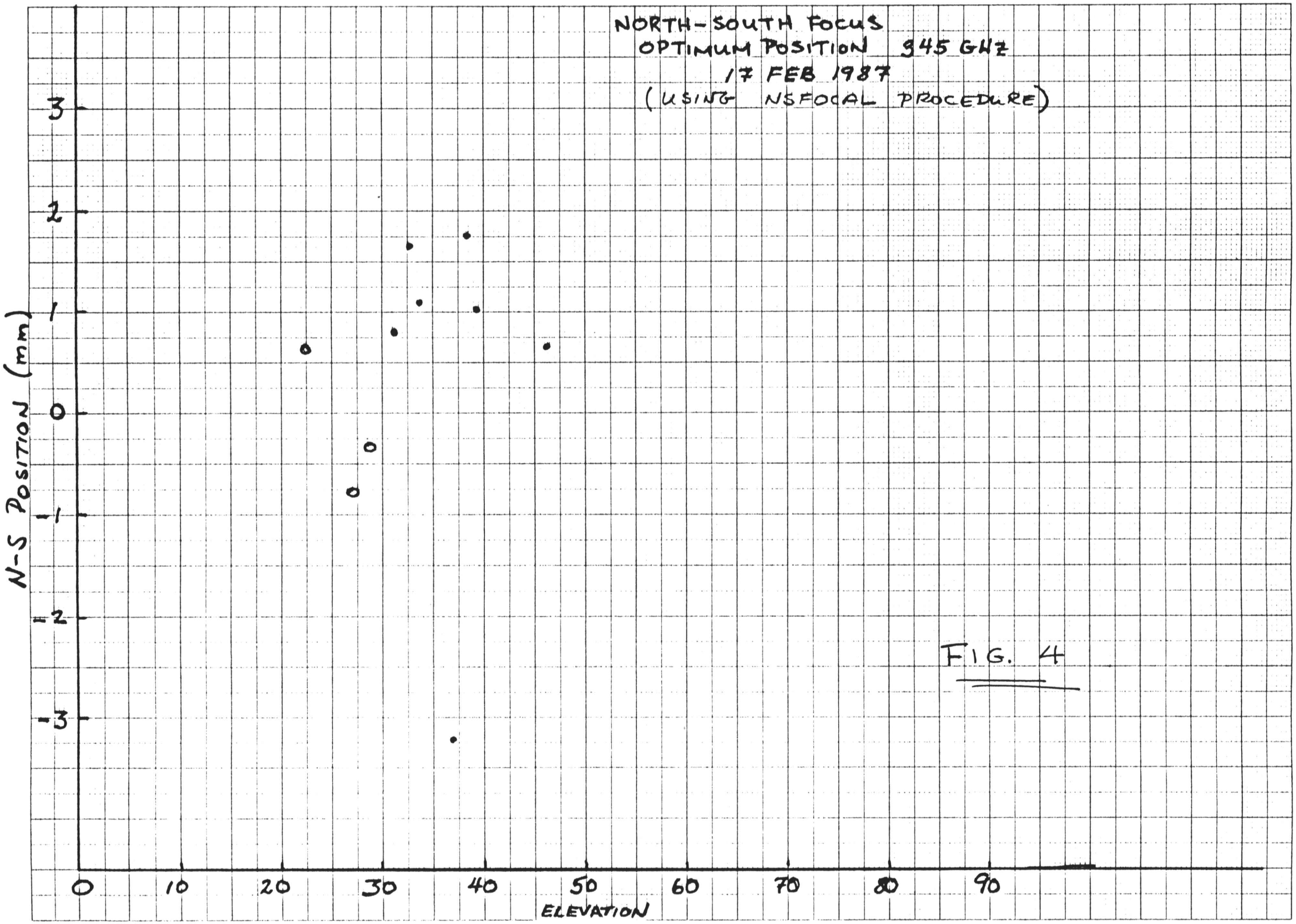
NORTH-SOUTH FOCUS
OPTIMUM POSITION 345 GHz
17 FEB 1987
(USING NSFOCAL PROCEDURE)
N-S POSITION (mm)
3
2
1
0
-1
-2
-3
0
10
20
30
40
50
60
70
80
90
ELEVATION

FIG. 4

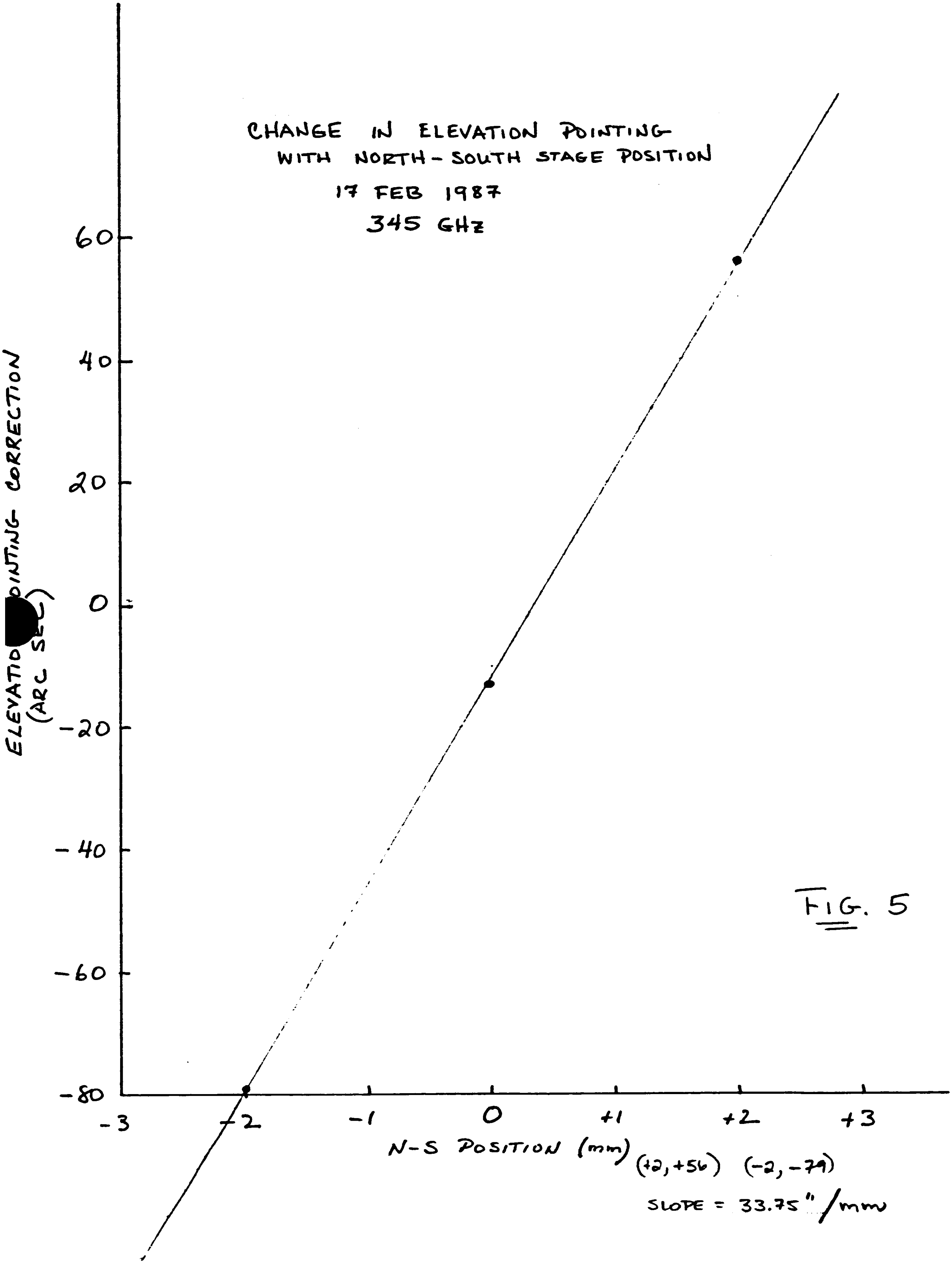

CHANGE IN ELEVATION POINTING
WITH NORTH-SOUTH STAGE POSITION
17 FEB 1987
345 GHz
60
40
20
0
-20
-40
-60
-80
ELEVATIO OINTING CORRECTION
(ARC SE)
-3
-2
-1
0
+1
+2
+3
N-S POSITION (mm)
(+2, +56) (-2, -79)
SLOPE = 33.75"/mm

FIG. 5

SKY NOISE AS A FUNCTION OF BEAM THROW

345 GHz 16 FEB 1987

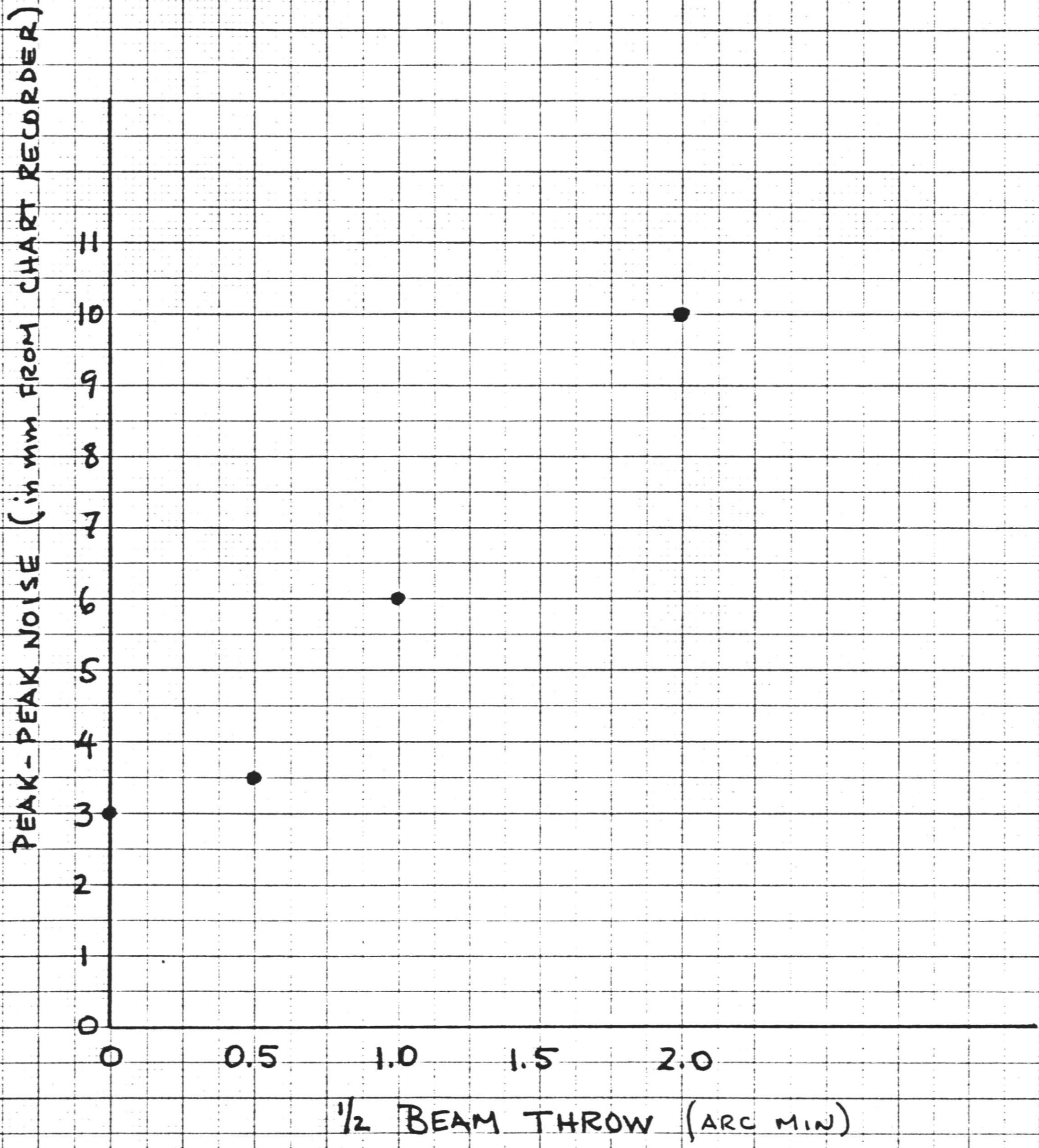

FIG. 6